

From High-Level Requirements to KPIs: Conformal Signal Temporal Logic Learning for Wireless Communications

Jiechen Chen, *Member, IEEE*, Michele Polese, *Member, IEEE*, and Osvaldo Simeone, *Fellow, IEEE*

Abstract—Softwarized radio access networks (RANs), such as those based on the Open RAN (O-RAN) architecture, generate rich streams of key performance indicators (KPIs) that can be leveraged to extract actionable intelligence for network optimization. However, bridging the gap between low-level KPI measurements and high-level requirements, such as quality of experience (QoE), requires methods that are both relevant, capturing temporal patterns predictive of user-level outcomes, and interpretable, providing human-readable insights that operators can validate and act upon. This paper introduces conformal signal temporal logic learning (C-STLL), a framework that addresses both requirements. C-STLL leverages signal temporal logic (STL), a formal language for specifying temporal properties of time series, to learn interpretable formulas that distinguish KPI traces satisfying high-level requirements from those that do not. To ensure reliability, C-STLL wraps around existing STL learning algorithms with a conformal calibration procedure based on the Learn Then Test (LTT) framework. This procedure produces a set of STL formulas with formal guarantees: with high probability, the set contains at least one formula achieving a user-specified accuracy level. The calibration jointly optimizes for reliability, formula complexity, and diversity through principled acceptance and stopping rules validated via multiple hypothesis testing. Experiments using the ns-3 network simulator on a mobile gaming scenario demonstrate that C-STLL effectively controls risk below target levels while returning compact, diverse sets of interpretable temporal specifications that relate KPI behavior to QoE outcomes.

Index Terms—Radio access networks, signal temporal logic, signal temporal logic learning, learn then test.

I. INTRODUCTION

A. Motivation

The wealth of data produced by modern wireless networks creates a unique opportunity to extract actionable intelligence that can drive network optimization, anticipate failures, and ensure quality of service guarantees [1]. In particular, network controllers in disaggregated architectures like O-RAN can aggregate rich streams of key performance indicators (KPIs), at the radio access network (RAN), including throughput,

J. Chen is with the Department of Engineering, King’s College London, London, WC2R 2LS, UK (email: jiechen.chen@kcl.ac.uk). M. Polese is with the Institute for Intelligent Networked Systems, Northeastern University, Boston, MA 02115 USA (email: m.polese@northeastern.edu). O. Simeone is with the Institute for Intelligent Networked Systems, Northeastern University London, One Portsoken Street, London, E1 8PH, UK (email: o.simeone@northeastern.edu).

This work was supported by the European Research Council (ERC) under the European Union’s Horizon Europe Programme (grant agreement No. 101198347), by an Open Fellowship of the EPSRC (EP/W024101/1), by the EPSRC project (EP/X011852/1), and by the U.S. NSF under grant TI-2449452.

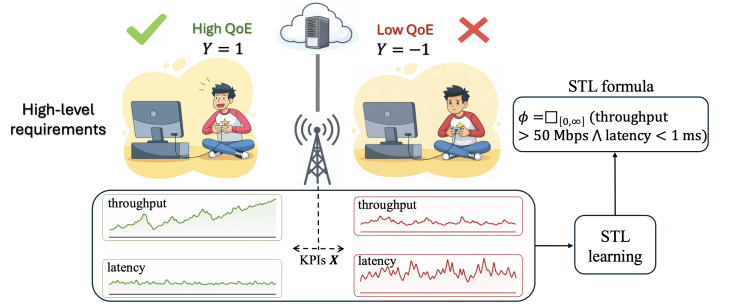


Fig. 1. From high-level requirements to KPI requirements: The radio access network (RAN) collects traces of KPIs such as throughput and latency over time. High-level QoE evaluations are provided by end users. The goal of this work is to infer interpretable properties of KPI traces that are predictive of whether high-level requirements are satisfied or not. These properties are expressed by the formal language signal temporal logic (STL), which provides tools to describe temporal constraints as time series.

latency, packet loss, and signal quality [2–4]. Beyond relevance, intelligence extracted from the RAN must also be *interpretable* [5–7], allowing network operators to understand *why* a decision was made either to validate decisions against domain expertise or to satisfy regulatory requirements.

However, extracting interpretable intelligence from RAN traces presents a challenge given the gap between the *low-level KPI measurements* readily available at the RAN and the *high-level behavioral requirements* that matter to network operators and end users (see Fig. 1). Explanations about QoE outcomes must be constructed from the only available data, namely low-level RAN KPI trace logs. This necessitates the development of novel interpretable mechanisms to bridge the semantic gap between QoE targets and RAN KPI traces.

Signal Temporal Logic (STL) offers a principled framework for expressing and learning interpretable temporal properties of time-series data [8, 9]. An STL formula such as

$$\square_{[0, \infty)}((\text{latency} < 100 \text{ ms}) \wedge \diamond_{[0, 5]}(\text{throughput} > 50 \text{ Mbps})) \quad (1)$$

provides a human-readable specification that directly relates KPI behavior to requirements. For example, the STL formula in (1) states that latency must always remain below 100 ms and (denoted as \wedge) throughput must exceed 50 Mbps at least once within every time slot consisting of a 5-TTI window. Unlike feature attributions from standard explainable AI methods such as SHAP or LIME [5], STL formulas constitute *formal specifications* that can be verified, composed, and directly translated into network policies.

That said, existing *STL learning* (STLL) methods, while effective at extracting candidate formulas from labeled data, provide no formal guarantees on the reliability of learned specifications [10, 11]. A formula that performs well on training data may fail to generalize, potentially leading to costly misclassifications in deployment. This limitation is particularly concerning in wireless communications, where network decisions based on unreliable predictions can degrade user experience or violate service level agreements (SLAs).

B. Related Work

1) *Signal temporal logic*: STL enables precise specification of temporal properties [8], and the quantitative semantics of STL, known as robustness, provide a real-valued measure indicating the degree to which a signal satisfies a formula [9, 11, 12]. This quantitative interpretation enables gradient-based optimization and serves as a natural loss function for learning [10].

While STL learning has been successfully applied in cyber-physical systems, robotics, and autonomous vehicles [13], its application to wireless communications remains largely unexplored. In particular, recent work has begun to explore STL formalisms for network verification and monitoring [14].

2) *Explainable AI for wireless communications*: The need for explainable AI (XAI) in wireless networks has been increasingly recognized as ML models are deployed for critical network functions [5, 6, 15, 16]. Several frameworks have been developed to provide interpretability specifically for AI-driven O-RAN control. These include EXPLORA [7], which uses attributed graphs to link DRL-based agent actions to wireless network context; XAI-on-RAN, which integrates GPU-accelerated explainability techniques for real-time operation [17]; as well as work on RAN slicing and resource allocation [18], anomaly detection using interpretable autoencoders [19], and energy efficiency optimization [20].

However, existing XAI methods for wireless predominantly rely on statistical attribution, and the application of formal specification languages to wireless network intelligence remains an open research direction.

3) *Conformal prediction and reliability guarantees*: Conformal prediction is a distribution-free framework for constructing prediction sets with guaranteed coverage [21, 22]. It has recently been applied to wireless communications for tasks including demodulation and neuromorphic wireless edge intelligence [23–26]. Reference [27] studied the problem of predictive monitoring based on STL and conformal prediction. The Learn Then Test (LTT) framework recasts risk control as multiple hypothesis testing, enabling control of general risk functions beyond miscoverage [28].

4) *QoE prediction*: Predicting user QoE from network-level measurements [29] was addressed in reference [30] for voice-over-IP (VoIP) systems, while reference [31] focused on predicting future virtual reality QoE levels in O-RAN networks. These approaches inherit the limitations of black-box models in terms of interpretability and statistical validity.

C. Main Contributions

This paper introduces *conformal STL learning* (C-STLL), a novel framework for extracting interpretable, reliability-guaranteed temporal specifications from wireless KPI traces. The main contributions are as follows:

- 1) **STL learning to wireless communications**: We demonstrate that STL provides a natural and effective formalism for expressing temporal properties of KPI traces that are predictive of high-level QoE requirements. Unlike black-box ML models, learned STL formulas are human-readable and verifiable.
- 2) **Conformal calibration for reliable specification learning**: We develop C-STLL, a calibration methodology that wraps around any STLL algorithm to produce a *set* of STL formulas with formal reliability guarantees (see Fig. 2). Specifically, C-STLL ensures that, with high probability, the returned set contains at least one formula achieving a target accuracy level. This is accomplished through a novel combination of sequential STL formula generation, acceptance rules based on complexity and diversity criteria, and multiple hypothesis testing via the Learn Then Test framework [28, 32, 33].
- 3) **Experimental validation**: We evaluate C-STLL using the ns-3 network simulator, modeling a mobile gaming scenario with realistic traffic patterns and network conditions. Experiments demonstrate that C-STLL successfully controls risk below specified tolerance levels while producing compact, diverse sets of interpretable STL formulas. Comparisons with ablated variants of the proposed framework confirm the importance of each component of the proposed framework.

The remainder of this paper is organized as follows. Section II reviews the syntax and semantics of STL. Section III formulates the STL learning problem and describes existing solution approaches. Section IV presents the proposed C-STLL framework, including the sequential generation procedure and the calibration methodology based on multiple hypothesis testing. Section V provides experimental results, and Section VI concludes the paper.

II. BACKGROUND: SIGNAL TEMPORAL LOGIC

Signal Temporal Logic (STL) is a formal language for specifying and analyzing the temporal properties of time-series data. In this section, we present the standard STL syntax together with quantitative metrics used to evaluate the degree of satisfaction of given STL properties.

A. STL Formulas

Let $\mathbf{X} = [\mathbf{x}_0, \mathbf{x}_1, \dots, \mathbf{x}_{T-1}]$ be a finite discrete-time trajectory with $\mathbf{x}_t = [x_{1,t}, \dots, x_{d,t}] \in \mathbb{R}^d$ denoting the system state at time t , where integer d is the dimension of the state. In wireless communications, each vector \mathbf{x}_t may represent a collection of KPIs extracted over transmission time intervals (TTIs) indexed as $t = 0, 1, \dots$, e.g., one entry $x_{i,t}$ of vector \mathbf{x}_t may report the throughput of some user and another entry, $x_{j,t}$, the latency of the user.

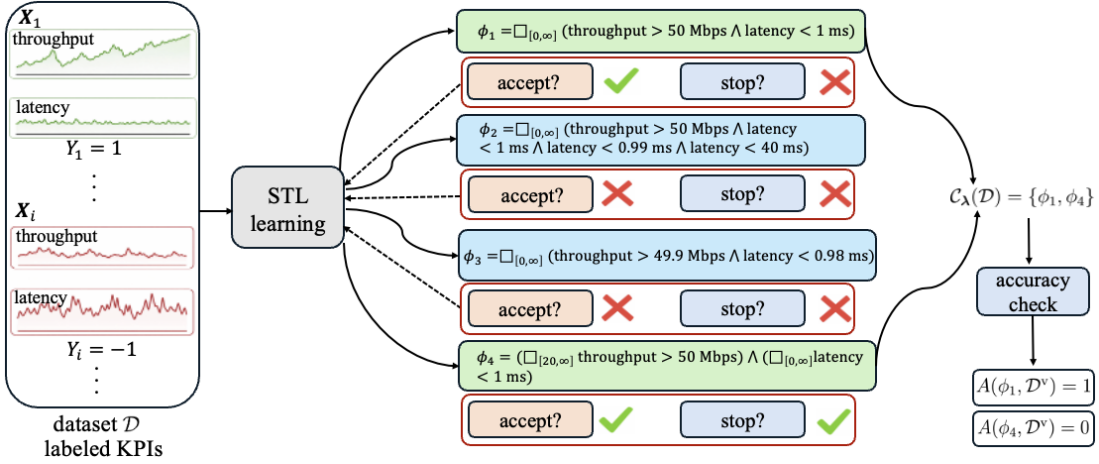


Fig. 2. Illustration of the proposed conformal STL learning (C-STLL) scheme. As illustrated in Fig. 1, KPI traces are labeled as $Y = 1$ or $Y = -1$ based on whether or not they correspond to settings in which positive or negative higher-level requirements are satisfied. Via any STLL algorithm [10], the dataset \mathcal{D} of labeled KPI traces can be leveraged to produce an STL formula ϕ , providing interpretable conditions on the KPI time series that are consistent with positive labels. However, this approach provides no guarantees on the reliability and accuracy of the formula ϕ . The proposed C-STLL wraps around any STLL procedure to produce a set of STL formulas with *reliability and quality assurance*. Through a sequential application of the STL algorithm, each newly learned formula is either accepted for inclusion in the set or rejected, and the process is continued or stopped, based on calibrated threshold-based procedures. In this example, formula ϕ_2 is rejected due to its high complexity, while ϕ_3 is rejected for being too similar to ϕ_1 , which is already in the set.

An STL formula ϕ specifies a property that time series \mathbf{X} may exhibit or not. Specifically, one writes

$$(\mathbf{X}, t) \models \phi, \quad (2)$$

if sequence \mathbf{X} satisfies property ϕ from time t onward, so the symbol \models reads “satisfies”. For example, a sequence of KPIs, \mathbf{X} , corresponding to nominal behavior of a radio access network may satisfy the property ϕ that the latency of a certain group of users does not drop below 1 ms for more than a given number of TTIs starting from some TTI t .

STL properties ϕ are built from atomic predicates of the form

$$\mu ::= \mathbf{a}^\top \mathbf{x} > b, \quad (3)$$

with $\mathbf{a} \in \mathbb{R}^d$ and $b \in \mathbb{R}$, where the symbol $::=$ is to be read as “is defined as”. Specifically, the basic STL property $(\mathbf{X}, t) \models \phi$ is equivalent to the condition $\mathbf{a}^\top \mathbf{x}_t > b$ requiring the predicate (3) to be valid for all times starting from t . As we will discuss below, more complex properties can be built from basic predicates of the form (3).

For example, consider the property that the throughput $x_{i,t}$ of a given user must be larger than a threshold $b = 50$ Mbit per second (Mbps). Using a “one-hot” vector \mathbf{a} with a single one in position i and all other zero entries, denoted as \mathbf{e}_i , this can be expressed as the STL property $(\mathbf{X}, t) \models (\mathbf{e}_i^\top \mathbf{x} = x_i > 50 \text{ Mbps})$.

More generally, STL formulas can be constructed by leveraging the *eventually* operator $\diamond_{[t_1, t_2]}$, the *always* operator $\square_{[t_1, t_2]}$, as well as logical operations such as AND and OR. In particular, using the eventually operator, the condition $(\mathbf{X}, t) \models \phi$ with the STL property

$$\phi ::= \diamond_{[t_1, t_2]} \mu \quad (4)$$

is true if the condition μ holds at *any* time $t' \in [t + t_1, t + t_2]$, i.e., in an interval of the form $[t_1, t_2]$ with time measured

starting from index t . In a similar way, using the *always* operator, the condition $(\mathbf{X}, t) \models \phi$ with the STL property

$$\phi ::= \square_{[t_1, t_2]} \mu \quad (5)$$

is valid if the property μ holds for *all* $t' \in [t + t_1, t + t_2]$. For instance, continuing the wireless example, the STL property $(\mathbf{X}, 0) \models \square_{[0, \infty]}(x_i > 50 \text{ Mbps})$ is true if the throughput $x_{i,t'}$ is no smaller than 50 Mbps for all TTIs starting at time index 0.

In broadest generality, formulas such as (4) and (5) can be composed recursively, making use also of logical operations, namely AND (\wedge) and OR (\vee). Specifically, one can recursively define an STL property via the rule

$$\phi ::= \mu \mid \wedge_{i=1}^n \phi_i \mid \vee_{i=1}^n \phi_i \mid \diamond_{[t_1, t_2]} \phi \mid \square_{[t_1, t_2]} \phi, \quad (6)$$

where μ is an atomic predicate (3), and each step of the recursion applies one of the options in (6), which are separated by a bar “|” following a standard convention [34].

For instance, consider the property for a given user that the throughput $x_{i,t}$ must be larger than 50 Mbit per second (Mbps) and the latency $x_{j,t}$ must be smaller than 1 ms for all TTIs starting at TTI t . The STL property

$$(\mathbf{X}, 0) \models \square_{[0, \infty]}(x_i > 50 \text{ Mbps} \wedge \diamond_{[0, 5]}(x_j \leq 1 \text{ ms})), \quad (7)$$

is true if for each TTI t starting from $t = 0$, the throughput is larger than 50 Mbps and the latency is no larger than 1 ms in at least one of 5 consecutive TTIs.

B. Robustness

STL is equipped with a robustness scores, which assign to each formula ϕ and signal \mathbf{X} a real-valued function $\rho(\mathbf{X}, \phi, t) \in \mathbb{R}$ that measures the degree to which ϕ is satisfied when the evaluation begins at time t [8]. By definition of

robustness measure, a signal satisfies the formula ϕ from time t if and only if its robustness is positive, i.e.,

$$(\mathbf{X}, t) \models \phi \iff \rho(\mathbf{X}, \phi, t) > 0, \quad (8)$$

and larger robustness values $\rho(\mathbf{X}, \phi, t)$ indicate stronger satisfaction.

For an atomic predicate μ in (3), the robustness is defined as

$$\rho(\mathbf{X}, \mu, t) = \mathbf{a}^\top \mathbf{x}_t - b. \quad (9)$$

Accordingly, the robustness is positive if $\mathbf{a}^\top \mathbf{x}_t > b$. When considering a general STL formula constructed via the rule (6), the robustness can be obtained by using the following rules. The robustness of the logical AND of more properties, $\phi = \bigwedge_{i=1}^n \phi_i$, is the minimum

$$\rho(\mathbf{X}, \bigwedge_{i=1}^n \phi_i, t) = \min_{i=1, \dots, n} \rho(\mathbf{X}, \phi_i, t), \quad (10)$$

since all properties $\{\phi_i\}_{i=1}^n$ must be satisfied; while for the logical-OR formula $\phi = \bigvee_{i=1}^n \phi_i$, the robustness is the maximum

$$\rho(\mathbf{X}, \bigvee_{i=1}^n \phi_i, t) = \max_{i=1, \dots, n} \rho(\mathbf{X}, \phi_i, t), \quad (11)$$

since the validity of any property ϕ_i is sufficient for the validity of the entire property ϕ . Finally, in a similar way, for the eventually operator, we have

$$\rho(\mathbf{X}, \diamond_{[t_1, t_2]} \phi, t) = \max_{t' \in [t+t_1, t+t_2]} \rho(\mathbf{X}, \phi, t'), \quad (12)$$

and for the always operator the robustness is

$$\rho(\mathbf{X}, \square_{[t_1, t_2]} \phi, t) = \min_{t' \in [t+t_1, t+t_2]} \rho(\mathbf{X}, \phi, t'). \quad (13)$$

III. LEARNING STL PROPERTIES

In this section, we discuss the problem of learning from labeled traces an interpretable prediction rule based on STL by following [10]. The goal is to infer a formal property, in the form of an STL formula ϕ , that lower-level traces \mathbf{X} satisfying higher-level requirements are likely to meet.

A. Formulating STL Learning

Consider a system in which traces \mathbf{X} can be collected that describe the evolution of the variables of interest, here the KPIs of a RAN. To each trace \mathbf{X} , an end user can potentially assign a binary label $Y \in \{1, -1\}$ indicating whether trajectory \mathbf{X} satisfies given higher-level requirements, $Y = 1$, or violates them, $Y = -1$. Henceforth, we will refer to a sequence \mathbf{X} labeled $Y = 1$ as *positive*, and to a sequence \mathbf{X} with $Y = -1$ as *negative*. As in Fig. 1, the higher-level requirements may refer to the QoE of end users when interacting with certain applications over the network.

We are interested in the problem of *STL learning* (STLL), where the goal is to infer an STL formula ϕ that can effectively distinguish between traces with positive and negative labels. Specifically, we would like to identify an STL formula ϕ that is likely to be satisfied by traces \mathbf{X} with positive labels, i.e., $(\mathbf{X}, 0) \models \phi$ if $Y = 1$, while being violated by traces with

negative labels, i.e., $(\mathbf{X}, 0) \not\models \phi$ if $Y = -1$. Note that the starting time is chosen as $t = 0$ by convention.

Accordingly, the classification decision \hat{Y} associated with an STL property ϕ is given by

$$\hat{Y} = \begin{cases} 1, & \text{if } (\mathbf{X}, 0) \models \phi, \\ -1, & \text{if } (\mathbf{X}, 0) \not\models \phi, \end{cases} \quad (14)$$

or equivalently in terms of robustness

$$\hat{Y} = \begin{cases} 1, & \text{if } \rho(\mathbf{X}, \phi, 0) > 0, \\ -1, & \text{if } \rho(\mathbf{X}, \phi, 0) < 0. \end{cases} \quad (15)$$

Accordingly, the robustness $\rho(\mathbf{X}, \phi, 0)$ serves as a logit in conventional binary classification.

The STLL problem is formulated as a supervised learning task. To this end, assume access to a labeled dataset $\mathcal{D} = \{(\mathbf{X}_i, Y_i)\}_{i=1}^{|\mathcal{D}|}$ in which each pair (\mathbf{X}_i, Y_i) is drawn i.i.d. from an underlying ground-truth distribution $P_{\mathbf{X}, Y}$ following the standard frequentistic learning framework (see e.g., [35]). The data distribution describes the current, ground-truth, relationship between the traces \mathbf{X} and the label Y .

Using (15), for each labeled pair $(\mathbf{X}, Y) \sim P_{\mathbf{X}, Y}$, the *classification margin*, given by the product $Y\rho(\mathbf{X}, \phi, 0)$, is positive if the STL formula correctly marks a trace \mathbf{X} as positive or negative; while a negative classification margin $Y\rho(\mathbf{X}, \phi, 0)$ indicates an incorrect classification decision. Accordingly, any non-increasing function of the classification margin can serve as a loss function for the STL problem (see, e.g., [35, Chapter 6]). Specifically, in [10], the shifted hinge loss

$$\ell(\phi, \mathbf{X}, Y) = \text{ReLU}(\beta - Y\rho(\mathbf{X}, \phi, 0)) - \gamma\beta \quad (16)$$

was adopted, where the hyperparameters $\beta > 0$ specifies the desired robustness margin and $\gamma > 0$ adjusts the trade-off in penalizing samples that already satisfy the margin.

Using the loss $\ell(\phi, \mathbf{X}, Y)$, for any given point distribution $P_{\mathbf{X}, Y}$, the goal is to find an STL rule ϕ that minimizes the population loss

$$L_P(\phi) = \mathbb{E}_{(\mathbf{X}, Y) \sim P_{\mathbf{X}, Y}}[\ell(\mathbf{X}, Y)], \quad (17)$$

where the average is evaluated over the joint distribution $P_{\mathbf{X}, Y}$ of input \mathbf{X} and target Y . The expected value in (17) is practically approximated using the dataset \mathcal{D} , yielding the training loss

$$L_{\mathcal{D}}(\phi) = \frac{1}{|\mathcal{D}|} \sum_{i=1}^{|\mathcal{D}|} \ell(\mathbf{X}_i, Y_i). \quad (18)$$

However, a direct optimization of the training loss $L_{\mathcal{D}}(\phi)$ over the STL formula ϕ is made difficult by the fact that the space of STL formulas is discrete.

B. Addressing the STL Learning Problem

In order to address the STLL problem of minimizing the training loss (18) over the STL formula ϕ , reference [10] introduced a relaxation-based method. Specifically, the STLL approach in [10] relaxes the discrete variables dictating the sequence of temporal operators and logical operations applied

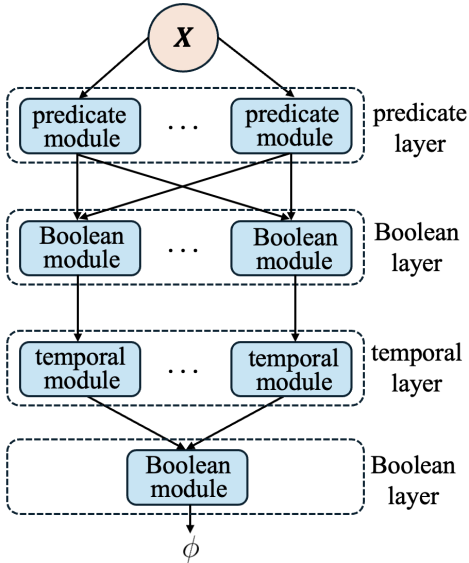


Fig. 3. An illustration of a parameterized template for the construction of an STL formula ϕ . In this example, the STL formula ϕ is constructed by the following steps: 1) a number of predicates μ , as in (3), are selected; 2) the predicates are combined via Boolean operators, either \wedge or \vee ; 3) temporal operators $\diamond_{[t_1, t_2]}$ or $\square_{[t_1, t_2]}$ are applied to the resulting partial STL formulas; and 4) another Boolean operator is used to combine the partial STL properties constructed at the previous steps. Each layer is specified by parameters that are optimized by addressing the STLL problem.

in the construction rule (6) to obtain the STL formula ϕ . To this end, reference [10] starts by assuming a template for the STL formula ϕ as a sequence of steps in the construction (6) of an STL rule. An example, adapted from [10], is shown in Fig. 3, in which the formula ϕ is constructed via the following steps: 1) a number of predicates μ , as in (3), are selected; 2) the predicates are combined via Boolean operators, which may be either \wedge or \vee ; 3) temporal operators, namely $\diamond_{[t_1, t_2]}$ or $\square_{[t_1, t_2]}$, are applied to the resulting partial STL formulas; and 4) another Boolean operator, either \wedge or \vee , is used to combine the partial STL properties constructed at the previous steps.

Accordingly, as illustrated in Fig. 3, a general template contains predicate layer, Boolean layers, and temporal layers. Therefore, templates such as that in Fig. 3 fully specify an STL property ϕ once a number of parameters are given, namely: (i) the variables a and b defining the atomic predicate of a predicate module; (ii) the binary variables determining which logical operator (AND or OR) is applied and which formulas constructed from previous steps are combined in a temporal module; (iii) the binary variables determining whether a temporal operator is “always” \square or “eventually” \diamond , as well as the corresponding interval bounds t_1 and t_2 , in a temporal module.

Minimizing the training loss $L_{\mathcal{D}}(\phi)$ over an STL formula ϕ following a given template thus requires optimizing over both continuous variables – namely a, b, t_1, t_2 – and discrete variables – i.e., the mentioned binary indicators. Reference [10] proposes relaxing the binary variables to probabilities so as to obtain a differentiable training loss, while adding regularizers to push optimized probabilities towards either 0 or 1. For completeness, more details on the STLL procedure

introduced in [10] can be found in Appendix A.

IV. CONFORMAL STL LEARNING

As discussed in the previous section, given a dataset \mathcal{D} , STLL methods obtain an STL formula ϕ that ideally distinguishes positive and negative sequences with minimal average error. However, being based on standard supervised learning methodologies, such techniques do not provide any formal, finite-sample, guarantee on the actual average loss obtained by the optimized formula ϕ . This can make the deployment of these methods in sensitive domains potentially problematic. In this section, we introduce *conformal STL learning* (C-STLL), a calibration methodology building on *sequential generation* and *multiple hypothesis testing*.

A. Reliable STL Learning via Sequential Generation

Via sequential generation, C-STLL constructs a *set* of candidate STL formulas using multiple runs of an STLL algorithm. We specifically adopt the STLL algorithm in [10], which was reviewed in Section III-B. As illustrated in Fig. 2, C-STLL calibrates an acceptance rule determining whether a formula generated via STLL is accepted for inclusion in the set, together with a stopping rule dictating when to stop generating. C-STLL leverages held-out data, and has the following aims: (i) to formally ensure that at least one high-accuracy STL formula is included in the set with sufficiently large probability, and (ii) to make a best effort at minimizing the complexity and at maximizing the diversity of the STLL formulas in the generated set.

C-STLL follows the general methodology of conformal language modeling [33], which is itself grounded in Pareto testing [32] and learn then test (LTT) [28]. In the following, we first describe the sequential generation of STL formulas via STLL and the accuracy requirement, and then we present C-STLL as a calibration methodology for acceptance and stopping rules.

Formally, given a dataset \mathcal{D} , C-STLL constructs a set of STL formulas $\mathcal{C}_{\lambda}(\mathcal{D})$ through multiple runs of STLL [10] via the following steps.

1) *Sequential Generation*: At each learning run $l = 1, 2, \dots$, STLL is applied to the dataset \mathcal{D} as described in Sec. III-A, obtaining a generally different formula ϕ_l . To ensure the nondeterminism of STLL, and thus the generation of different STL formulas, we adopt an ensembling methodology based on randomizing initialization and mini-batch selection for stochastic gradient descent over the trainable parameters, as in deep ensembles [36]. An alternative approach may treat the STL parameters as random variables and sampling from a learned posterior distribution [37].

C-STLL includes formula ϕ_l in set $\mathcal{C}_{\lambda}(\mathcal{D})$ according to an *inclusion rule* $I_{\lambda}(\mathcal{D}, \phi_1, \dots, \phi_l)$, to be designed:

$$I_{\lambda}(\mathcal{D}, \phi_1, \dots, \phi_l) = \begin{cases} 1, & \text{if } \phi_l \in \mathcal{C}_{\lambda}(\mathcal{D}), \\ 0, & \text{otherwise.} \end{cases} \quad (19)$$

C-STLL stops when a stopping indicator $S_\lambda(\mathcal{D}, \phi_1, \dots, \phi_l)$, to be designed, returns 1, while proceeding to the next run $l + 1$ otherwise:

$$S_\lambda(\mathcal{D}, \phi_1, \dots, \phi_l) = \begin{cases} 1, & \text{if a stopping condition is satisfied,} \\ 0, & \text{otherwise.} \end{cases} \quad (20)$$

Acceptance rule $I_\lambda(\mathcal{D}, \phi_1, \dots, \phi_l)$ and stopping rule $S_\lambda(\mathcal{D}, \phi_1, \dots, \phi_l)$ generally depend on a vector of hyperparameters λ , as introduced in the next subsection.

2) *Reliability Requirements*: C-STLL designs the hyperparameter λ of the acceptance and stopping rule with the aim of ensuring a reliability requirement for the set $\mathcal{C}_\lambda(\mathcal{D})$, while also accounting for complexity and diversity of the formulas in set $\mathcal{C}_\lambda(\mathcal{D})$. The reliability condition is formalized as follows. Given an STL formula ϕ , any new trace \mathbf{X} can be classified as positive ($\hat{Y} = 1$) or negative ($\hat{Y} = -1$) based on (14), or equivalently (15). Given a validation dataset \mathcal{D}^v , we wish to impose that the fraction of correctly classified samples is larger than a user-defined threshold φ , i.e.,

$$\frac{1}{|\mathcal{D}^v|} \sum_{i=1}^{|\mathcal{D}^v|} \mathbb{1}(\hat{Y}_i = Y_i) > \varphi, \quad (21)$$

where $\mathbb{1}(\cdot)$ is the indicator function ($\mathbb{1}(\text{true}) = 1$ and $\mathbb{1}(\text{false}) = 0$). Accordingly, we define the accuracy indicator for an STL formula ϕ as

$$A(\phi, \mathcal{D}^v) = \begin{cases} 1, & \text{if } \frac{1}{|\mathcal{D}^v|} \sum_{i=1}^{|\mathcal{D}^v|} \mathbb{1}(\hat{Y}_i = Y_i) > \varphi, \\ 0, & \text{otherwise,} \end{cases} \quad (22)$$

so that $A(\phi, \mathcal{D}^v) = 1$ indicates that the STL formula ϕ is sufficiently accurate, while $A(\phi, \mathcal{D}^v) = 0$ signals the unreliability of formula ϕ .

The joint distribution $P_{\mathcal{D}\mathcal{D}^v}$ in practice captures the variability of the relationship between KPI traces \mathbf{X} and high-level labels Y across the tasks of interest. To formalize this, we introduce an indicator τ for a task of interest, corresponding, e.g., to some users, network conditions, and QoE requirements. Each pair $(\mathcal{D}, \mathcal{D}^v)$ of datasets pertains to a particular task τ . We model the task $\tau \sim P_\tau$ as a random variable with an unknown distribution P_τ , while the datasets $\mathcal{D} = \{(\mathbf{X}_i, Y_i)\}_{i=1}^{|\mathcal{D}|}$ and $\mathcal{D}^v = \{(\mathbf{X}_i, Y_i)\}_{i=1}^{|\mathcal{D}^v|}$ contain i.i.d. data from an unknown task-specific distribution $P_{\mathbf{X}, Y|\tau}$. Accordingly, the joint distribution of the dataset pair $(\mathcal{D}, \mathcal{D}^v)$ is given by the mixture

$$P_{\mathcal{D}\mathcal{D}^v} = \int P_\tau P_{\mathcal{D}|\tau} P_{\mathcal{D}^v|\tau} d\tau, \quad (23)$$

where the task indicator τ is marginalized over P_τ , and $P_{\mathcal{D}|\tau}$ and $P_{\mathcal{D}^v|\tau}$ represent the i.i.d. distributions obtained from distribution $P_{\mathbf{X}, Y|\tau}$.

Using this accuracy function, we define the risk associated with the choice of hyperparameter λ as the probability that there is no sufficiently accurate STL formula ϕ in set $\mathcal{C}_\lambda(\mathcal{D})$, i.e.,

$$R(\lambda) = \Pr\{\nexists \phi \in \mathcal{C}_\lambda(\mathcal{D}) : A(\phi, \mathcal{D}^v) = 1\}. \quad (24)$$

In interpreting the probability in (24), we view the dataset pair $(\mathcal{D}, \mathcal{D}^v)$ as random, following some unknown joint distribution

$P_{\mathcal{D}\mathcal{D}^v}$. Our design goal is to identify a hyperparameter λ^* , which guarantees that the risk is controlled with high probability, i.e.,

$$\Pr(R(\lambda^*) < \epsilon) \geq 1 - \delta, \quad (25)$$

where the probability is over any randomness associated with the optimization of the hyperparameters λ^* . By (25), the risk of the generated set $\mathcal{C}_\lambda(\mathcal{D})$ must be smaller than ϵ with probability larger than $1 - \delta$.

B. Conformal STL Learning

As discussed, C-STLL builds the set $\mathcal{C}_\lambda(\mathcal{D})$ sequentially, and we define henceforth as $\mathcal{C}_{\lambda, l}(\mathcal{D})$ the current set at iteration l , with the initial set $\mathcal{C}_{\lambda, 0}(\mathcal{D})$ being empty.

Acceptance rule: At each run l , C-STLL accepts an STL formula ϕ_l into the set $\mathcal{C}_{\lambda, l}(\mathcal{D})$, setting $I_\lambda(\mathcal{D}, \phi_1, \dots, \phi_l) = 1$, if the formula is of sufficiently low complexity and sufficiently diverse relative to the previously accepted formulas. To elaborate, let $H(\phi_l)$ denote a function that maps the learned STL ϕ_l to a scalar quantity measuring its complexity. A less complex formula is generally more interpretable, and thus more useful to relate KPI traces to high-level requirements. We specifically adopt the number of operations as the measure of complexity $H(\phi_l)$ [38]. The candidate formula ϕ_l is deemed of sufficiently low complexity if the measure $H(\phi_l)$ is smaller than a threshold λ_1 , i.e.,

$$H(\phi_l) < \lambda_1. \quad (26)$$

Quality alone, however, is insufficient for constructing an informative set of formulas, since the learned formulas may be structurally similar. To avoid admitting redundant formulas, each candidate is additionally compared with those already in set $\mathcal{C}_{\lambda, l}(\mathcal{D})$ by using a distance measure, which is designed to detect duplicates and promote structural diversity. A new candidate ϕ_l is deemed to be sufficiently diverse from previous included formulas if the distance $D(\phi_l, \phi)$ between ϕ_l and all of the previously accepted formula $\phi \in \mathcal{C}_{\lambda, l-1}(\mathcal{D})$ is larger than a threshold λ_2 , i.e.,

$$D(\phi_l, \phi) > \lambda_2, \text{ for all } \phi \in \mathcal{C}_{\lambda, l-1}(\mathcal{D}). \quad (27)$$

As distance function, we follow [39] and measure semantic dissimilarity by comparing the robustness scores of the two formulas on the dataset \mathcal{D} as

$$D(\phi_l, \phi) = \sigma\left(\frac{1}{|\mathcal{D}|} \sum_{i=1}^{|\mathcal{D}|} \left| |\rho(\mathbf{X}_i, \phi_l, 0)| - |\rho(\mathbf{X}_i, \phi, 0)| \right| \right). \quad (28)$$

The use of the sigmoid function $\sigma(\cdot) = (1 + e^{-\cdot})^{-1}$ in (28) ensures that the distance is normalized between 0 and 1. Two STL formulas that behave similarly across traces in dataset \mathcal{D} will produce nearly identical robustness values, leading to a small distance (28).

When a candidate satisfies both the complexity and diversity criteria, it is accepted into the set $\mathcal{C}_{\lambda, l}(\mathcal{D})$, i.e., the acceptance function is given by

$$I_\lambda(\mathcal{D}, \phi_1, \dots, \phi_l) = \mathbb{1}(H(\phi_l) < \lambda_1 \text{ and } D(\phi_l, \phi) > \lambda_2, \text{ for all } \phi \in \mathcal{C}_{\lambda, l-1}(\mathcal{D})). \quad (29)$$

Algorithm 1: Conformal STL Learning (C-STLL) —
test time

- 1: **Input:** Labeled dataset \mathcal{D}
 - 2: **Initialization:** The initial set is empty $\mathcal{C}_{\lambda,0}(\mathcal{D}) = \{\}$
 - 3: **for** $l = 1, 2, \dots, L_{\max}$ **do**
 - 4: Run STLL [10] on dataset \mathcal{D} to learn an STL formula ϕ_l
 - 5: **if** $H(\phi_l) < \lambda_1$ and $D(\phi_l, \phi) > \lambda_2$ for all $\phi \in \mathcal{C}_{\lambda,l-1}(\mathcal{D})$
 - 6: Add ϕ_l to the set $\mathcal{C}_{\lambda,l}(\mathcal{D})$
 - 7: **if** $F(\mathcal{C}_{\lambda,l}(\mathcal{D})) > \lambda_3$
 - 8: Exit the for loop
 - 9: **end if**
 - 10: **end for**
 - 11: **Output:** Set $\mathcal{C}_{\lambda}(\mathcal{D}) = \mathcal{C}_{\lambda,l}(\mathcal{D})$
-

Accordingly, the set is updated as

$$\mathcal{C}_{\lambda,l}(\mathcal{D}) = \begin{cases} \mathcal{C}_{\lambda,l-1}(\mathcal{D}) \cup \{\phi_l\}, & \text{if } I_{\lambda}(\mathcal{D}, \phi_1, \dots, \phi_l) = 1, \\ \mathcal{C}_{\lambda,l-1}(\mathcal{D}), & \text{otherwise.} \end{cases} \quad (30)$$

Stopping Rule: The sequential generation process is run for at most L_{\max} times, and may terminate early if the evolving set is assessed to be of high enough quality. To formalize the resulting stopping function $S_{\lambda}(\mathcal{D}, \phi_1, \dots, \phi_l)$ in (20), we define a set-based quality function $F(\mathcal{C}_{\lambda,l}(\mathcal{D}))$ for the set $\mathcal{C}_{\lambda,l}(\mathcal{D})$. Specifically, we define the quality of any STL formula ϕ_l as an increasing function of its average robustness on the dataset \mathcal{D} as

$$Q(\phi_l) = \sigma\left(\frac{1}{|\mathcal{D}|} \sum_{i=1}^{|\mathcal{D}|} \rho(\mathbf{X}_i, \phi_l, 0)\right), \quad (31)$$

where the sigmoid function again ensures a normalized measure in the interval $[0, 1]$. The set-based quality function $F(\mathcal{C}_{\lambda,l}(\mathcal{D}))$ is then defined as the average

$$F(\mathcal{C}_{\lambda,l}(\mathcal{D})) = \frac{1}{|\mathcal{C}_{\lambda,l}(\mathcal{D})|} \sum_{\phi \in \mathcal{C}_{\lambda,l}(\mathcal{D})} Q(\phi). \quad (32)$$

C-STLL stops generating STL formulas at the earliest iteration l for which we have the inequality

$$F(\mathcal{C}_{\lambda,l}(\mathcal{D})) > \lambda_3, \quad (33)$$

where λ_3 is a threshold. The overall C-STLL procedure is summarized in Algorithm 1. The vector of hyperparameters $\boldsymbol{\lambda} = (\lambda_1, \lambda_2, \lambda_3)$, which encompass the complexity threshold λ_1 (26), the diversity threshold λ_2 (27), and the early-stopping threshold λ_3 (33) are optimized during a preliminary calibration phase, which is discussed next.

C. Reliable Hyperparameter Optimization via Multiple Hypothesis Testing

As discussed in Sec. IV-A, C-STLL aims at identifying hyperparameters $\boldsymbol{\lambda}^*$ that satisfy the reliability requirement (25), while attempting to introduce STL formulas with low complexity and to maintain diversity. To this end, C-STLL

carries out an offline calibration procedure based on calibration data encompassing examples of dataset pairs $(\mathcal{D}, \mathcal{D}^v)$ from different tasks. Following the setting described in Section IV-A2, we assume the availability of a calibration dataset $\mathcal{D}^{\text{cal}} = \{(\mathcal{D}_k, \mathcal{D}_k^v)\}_{k=1}^{|\mathcal{D}^{\text{cal}}|}$ consisting of pairs $(\mathcal{D}_k, \mathcal{D}_k^v)$ of training and validation datasets drawn i.i.d. from the dataset distribution $P_{\mathcal{D}\mathcal{D}^v}$. Accordingly, each pair $(\mathcal{D}_k, \mathcal{D}_k^v)$ corresponds to an independently generated task $\tau_k \sim P_{\tau}$. C-STLL uses the calibration dataset \mathcal{D}^{cal} to select hyperparameter $\boldsymbol{\lambda}^*$ so that the condition (25) is satisfied, where the outer probability is taken over the calibration dataset \mathcal{D}^{cal} .

To this end, C-STLL follows the LTT methodology [28] by specifically adopting Pareto testing [32]. In LTT, one starts by identifying a discrete subset Λ of configurations for the hyperparameter $\boldsymbol{\lambda}$. This can be done via a standard grid or through any optimization algorithm using prior information or separate data. For each hyperparameter $\boldsymbol{\lambda} \in \Lambda$, LTT tests the null hypothesis \mathcal{H}_{λ} that the true risk (24) is above the target uncertainty level ϵ , i.e.,

$$\mathcal{H}_{\lambda} : R(\boldsymbol{\lambda}) \geq \epsilon. \quad (34)$$

Rejecting the null hypothesis \mathcal{H}_{λ} identifies hyperparameter $\boldsymbol{\lambda}$ yielding reliable performance as measured by the accuracy indicator (22).

Using the calibration data \mathcal{D}^{cal} , for each hyperparameter $\boldsymbol{\lambda} \in \Lambda$, we evaluate the empirical risk $\hat{R}(\boldsymbol{\lambda}, \mathcal{D}^{\text{cal}})$ as

$$\hat{R}(\boldsymbol{\lambda}, \mathcal{D}^{\text{cal}}) = \frac{1}{|\mathcal{D}^{\text{cal}}|} \sum_{k=1}^{|\mathcal{D}^{\text{cal}}|} \mathbb{1}\{\nexists \phi \in \mathcal{C}_{\lambda}(\mathcal{D}_k) : A(\phi, \mathcal{D}_k^v) = 1\}, \quad (35)$$

which corresponds to an unbiased estimate of the true risk $R(\boldsymbol{\lambda})$ in (24). Accordingly, if the null hypothesis \mathcal{H}_{λ} holds, the estimate (35) will tend to be larger than ϵ . More precisely, let $b(|\mathcal{D}^{\text{cal}}|, \epsilon)$ denote a binomial random variable with sample size $|\mathcal{D}^{\text{cal}}|$ and success probability ϵ . A valid p-value for the hypothesis \mathcal{H}_{λ} in (34) is given by [33]

$$p(\boldsymbol{\lambda}) = \Pr(b(|\mathcal{D}^{\text{cal}}|, \epsilon) \leq |\mathcal{D}^{\text{cal}}| \hat{R}(\boldsymbol{\lambda}, \mathcal{D}^{\text{cal}})), \quad (36)$$

in the sense that we have the inequality $\Pr(p(\boldsymbol{\lambda}) \leq \delta | \mathcal{H}_{\lambda}) \leq \delta$ for all probability δ .

Using the p-values $\{p(\boldsymbol{\lambda})\}_{\boldsymbol{\lambda} \in \Lambda}$, LTT applies a family-wise error rate (FWER) multiple hypothesis testing (MHT) procedure to obtain a subset $\Lambda_{\text{valid}} \subseteq \Lambda$ with the property

$$\Pr(\exists \boldsymbol{\lambda} \in \Lambda_{\text{valid}} : R(\boldsymbol{\lambda}) \geq \epsilon) \leq \delta. \quad (37)$$

If the set Λ_{valid} is empty, we select the solution $\boldsymbol{\lambda}^* = [\lambda_1 = \infty, \lambda_2 = 0, \lambda_3 = \infty]^T$, which allows the set $\mathcal{C}_{\lambda}(\mathcal{D})$ to include all L_{\max} STL formulas. Otherwise, using any configuration in subset Λ_{valid} guarantees the reliability condition (25) by the FWER property (37). In C-STLL, we select the hyperparameter $\boldsymbol{\lambda}^* \in \Lambda_{\text{valid}}$ that minimizes the empirical set size, i.e.,

$$\boldsymbol{\lambda}^* = \arg \min_{\boldsymbol{\lambda} \in \Lambda_{\text{valid}}} \frac{1}{|\mathcal{D}^{\text{cal}}|} \sum_{k=1}^{|\mathcal{D}^{\text{cal}}|} |\mathcal{C}_{\lambda}(\mathcal{D}_k)|. \quad (38)$$

As for the FWER procedure, in order to efficiently search the set of candidates Λ , we use the Pareto Testing procedure

Algorithm 2: Conformal STL Learning (C-STLL) — calibration phase

- 1: **Input:** Calibration dataset \mathcal{D}^{cal} , set Λ , risk tolerance ϵ , error level δ
 - 2: **Initialization:** Initialize the reliable set as empty
 $\Lambda_{\text{valid}} = \{\}$
 - 3: **for** $\lambda \in \Lambda$ **do**
 - 4: Evaluate the empirical risk $\hat{R}(\lambda, \mathcal{D}^{\text{cal}})$ using (35)
 - 5: Compute the p-value $p(\lambda)$ for hypothesis \mathcal{H}_λ using (36)
 - 6: **end for**
 - 7: Apply LTT procedure on $\{p(\lambda)\}_{\lambda \in \Lambda}$ to obtain a subset $\Lambda_{\text{valid}} \subseteq \Lambda$ satisfying the FWER guarantee (37) (see Appendix B)
 - 8: **if** Λ_{valid} is empty
 - 9: Set $\lambda^* = [\lambda_1 = \infty, \lambda_2 = 0, \lambda_3 = \infty]^\top$
 - 10: **else**
 - 11: Select $\lambda^* \in \Lambda_{\text{valid}}$ that minimizes the empirical average set size as in (38)
 - 12: **end if**
 - 13: **Output:** Calibrated hyperparameter λ^*
-

from [32]. Pareto Testing exploits structure in Λ by first using a proportion of the dataset \mathcal{D}^{cal} to approximate the Pareto-optimal frontier in two-dimensional space, and by then iteratively validating promising configurations using fixed-sequence testing [40] on the remaining calibration data. Details can be found in Appendix B.

D. Theoretical Guarantees

Given its reliance on LTT, C-STLL guarantees the target reliability condition (25).

Theorem 1 (Reliability of C-STLL via LTT). *By setting the hyperparameter vector λ^* as described in Algorithm 2, the risk of the set $\mathcal{C}_{\lambda^*}(\mathcal{D})$ constructed via C-STLL as in Algorithm 1 satisfies the inequality (25).*

Proof. The proof is provided for completeness in the Appendix C. \square

V. EXPERIMENTS

In this section, we provide numerical results to demonstrate the effectiveness of the proposed C-STLL calibration methodology.

A. Setting

Throughout this section, we adopt the network simulator ns-3¹ to model a single gaming user communicating with a remote host over a wireless network (see Fig. 1). Bidirectional user datagram protocol (UDP) traffic is generated to emulate interactive gaming, while optional background users introduce network congestion. The *latency* KPI is defined as the one-way end-to-end delay of successfully received gaming

packets, averaged over uplink and downlink. The *backlog* KPI represents the number of user-side queued UDP packets awaiting transmission. Each trace \mathbf{X} consists of latency and backlog KPIs collected over 61 time steps, which corresponds to uniformly spaced observations over a real time observation of 13s.

We consider two different labeling strategies, with the first relying on a ground-truth STL formula, and the second mimicking a high-level QoE assessment. The first approach is included for reference, as it makes it possible to compare true and estimated STL formulas directly.

In the first approach, a trace is labeled as positive ($Y = 1$) if the latency remains below a threshold T_1 over all time steps, while the backlog is below a threshold T_2 during the final 5 time steps; otherwise, it is labeled as negative ($Y = -1$). This labeling approach has the advantage of providing a ground-truth STL formula, namely

$$\begin{aligned} \phi^{\text{true}} &= \square_{[0,60]}(\text{latency} < T_1 \text{ ms}) \\ &\wedge \square_{[56,60]}(\text{backlog} < T_2 \text{ kilobyte}), \end{aligned} \quad (39)$$

facilitating evaluation. We specifically use the threshold pairs $(T_1, T_2) = (100, 30), (110, 28), (120, 26), (130, 24)$, and $(140, 32)$ to label the entire dataset, corresponding to five distinct tasks.

We also consider a labeling setting mimicking the assessment of QoE levels from the end user (see Fig. 1). To this end, we adopt an LLM-as-a-judge approach [41, 42], whereby an LLM (ChatGPT5.1) is used to assign QoE labels based on the temporal evolution of latency and backlog. This is done by using the following prompt: “*You are a gaming user communicating with a remote host over a wireless network. The attached file contains KPIs including latency and backlog over 61 time steps. Evaluate the QoE according to one of the following five QoE definitions: (i) latency-dominant QoE, prioritizing consistently low latency; (ii) backlog-dominant QoE, prioritizing low queue backlog; (iii) balanced QoE, requiring both low latency and low backlog; (iv) burst-tolerant QoE, allowing short-term spikes in latency or backlog but penalizing sustained degradation; and (v) strict QoE, penalizing any persistent latency or backlog increase. Label each example with $Y = 1$ corresponding to high QoE and $Y = -1$ to low QoE.*”

Each training dataset \mathcal{D} contains 5,000 examples, and each validation set \mathcal{D}^v containing 1,000 examples. Given five tasks, each dataset pair $(\mathcal{D}, \mathcal{D}^v)$ is generated by first uniformly sampling a task τ , and then sampling from the labeled data corresponding to this task. We generate 100 calibration data pairs $(\mathcal{D}, \mathcal{D}^v)$, with 50 pairs used for Pareto testing, and the remaining 50 used for fixed-sequence testing (see Section IV-C).

B. Implementation

We adopt the STLL method in [10], which learns an STL formula via neural network-based optimization, as explain in Section III-B and Appendix A. We follow a template similar to Fig. 3, with six predicate modules at the input layer, followed by six temporal modules and a single Boolean

¹The simulator is available at <https://www.nsnam.org/>.

TABLE I
EXAMPLES OF LEARNED STL FORMULA SETS WITH CONVENTIONAL STLL [10] AND WITH VARIANTS OF THE PROPOSED C-STLL CALIBRATION SCHEMES GIVEN THE SAME TRAINING DATASET \mathcal{D} (TRUE LABELING STL FORMULA (39) WITH $T_1 = 100$ AND $T_2 = 30$).

Scheme	Learned STL Formula Set $\mathcal{C}_{\lambda^*}(\mathcal{D})$	Accuracy
STLL	$\phi = \square_{[24,39]}(\text{latency} < 21) \wedge \square_{[1,57]}(\text{backlog} < 59) \wedge \square_{[29,30]}(\text{latency} < 66) \wedge \square_{[11,42]}(\text{backlog} > 3)$	$\phi : 65\%$
C-STLL	$\{\phi_1 = \square_{[20,31]}(\text{latency} < 137) \wedge \square_{[25,60]}(\text{backlog} < 55),$ $\phi_2 = \diamond_{[11,40]}(\text{backlog} > 3) \wedge \square_{[0,55]}(\text{latency} < 30) \}$	$\phi_1 : 96.9\%$, $\phi_2 : 85\%$
C-STLL with stopping rule only	$\{\phi_1 = \square_{[19,49]}(\text{backlog} < 64),$ $\phi_2 = \diamond_{[19,33]}(\text{latency} < 154) \vee \square_{[9,48]}(\text{latency} < 22),$ $\phi_3 = \diamond_{[13,35]}(\text{backlog} > 60) \vee \diamond_{[14,45]}(\text{latency} < 20),$ $\phi_4 = \diamond_{[11,60]}(\text{backlog} < 4) \vee \square_{[13,38]}(\text{backlog} < 63),$ $\phi_5 = \square_{[5,29]}(\text{backlog} < 81),$ $\phi_6 = \diamond_{[18,32]}(\text{backlog} > 16) \wedge \diamond_{[24,54]}(\text{backlog} > 11) \wedge \diamond_{[0,33]}(\text{backlog} < 45),$ $\phi_7 = \square_{[15,36]}(\text{latency} < 14) \wedge \diamond_{[17,53]}(\text{backlog} < 24),$ $\phi_8 = \square_{[25,29]}(\text{latency} < 27),$ $\phi_9 = \square_{[0,33]}(\text{backlog} > 11) \vee \square_{[8,46]}(\text{backlog} > 21),$ $\phi_{10} = \square_{[15,38]}(\text{backlog} > 2) \wedge \square_{[18,29]}(\text{latency} < 28) \}$	$\phi_1 : 84.1\%$, $\phi_2 : 84.1\%$, $\phi_3 : 52.7\%$, $\phi_4 : 57.5\%$, $\phi_5 : 84.1\%$, $\phi_6 : 81.3\%$, $\phi_7 : 47.3\%$, $\phi_8 : 76.8\%$, $\phi_9 : 52.7\%$, $\phi_{10} : 71.9\%$
C-STLL with complexity check and stopping rule	$\{\phi_1 = \diamond_{[23,45]}(\text{backlog} > 2) \wedge \square_{[21,39]}(\text{backlog} < 75),$ $\phi_2 = \diamond_{[24,39]}(\text{backlog} > 8) \wedge \square_{[27,46]}(\text{latency} < 32),$ $\phi_3 = \diamond_{[18,32]}(\text{latency} < 17) \wedge \diamond_{[26,52]}(\text{backlog} > 4),$ $\phi_4 = \diamond_{[27,33]}(\text{backlog} < 45),$ $\phi_5 = \diamond_{[17,47]}(\text{backlog} > 12) \wedge \diamond_{[1,35]}(\text{backlog} < 73),$ $\phi_6 = \diamond_{[1,44]}(\text{latency} < 17) \wedge \diamond_{[13,52]}(\text{backlog} > 13),$ $\phi_7 = \square_{[25,54]}(\text{latency} < 20) \wedge \diamond_{[5,36]}(\text{backlog} > 6) \}$	$\phi_1 : 84.1\%$, $\phi_2 : 78.6\%$, $\phi_3 : 53.8\%$, $\phi_4 : 82.6\%$, $\phi_5 : 52.7\%$, $\phi_6 : 57.7\%$, $\phi_7 : 48.1\%$
C-STLL with diversity check and stopping rule	$\{\phi_1 = \square_{[24,51]}(\text{latency} < 32) \wedge \diamond_{[9,46]}(\text{latency} > 7) \wedge \square_{[13,37]}(\text{backlog} > 369) \wedge \square_{[4,36]}(\text{latency} < 31)$ $\phi_2 = \square_{[1,53]}(\text{latency} < 29) \vee \diamond_{[0,58]}(\text{latency} < 28),$ $\phi_3 = \diamond_{[11,45]}(\text{latency} < 179) \wedge \square_{[19,55]}(\text{backlog} > 48) \wedge \square_{[23,56]}(\text{latency} > 10) \wedge \diamond_{[25,54]}(\text{backlog} > 195) \wedge \diamond_{[0,52]}(\text{latency} < 101) \wedge \square_{[9,32]}(\text{backlog} > 189) \}$	$\phi_1 : 70.6\%$, $\phi_2 : 83.9\%$, $\phi_3 : 83.9\%$

module as the output layer. Following the recommendations in [10], the learning rate is set to 0.1, the batch size to 512, and the number of training epochs to 5, and in the loss function (16), we set $\beta = 0.1$ and $\gamma = 0.01$. The grid Λ contains all threshold tuples $(\lambda_1, \lambda_2, \lambda_3)$ with $\lambda_1 \in \{0.33, 0.5, 0.67\}$, $\lambda_2 \in \{0.50, 0.52, 0.54, 0.56, 0.58\}$, and $\lambda_3 \in \{0.3, 0.4, 0.5, 0.6, 0.7\}$. These ranges were chosen based on preliminary experiments to identify regions with meaningful variation in risk and set size over separate data generated in the same way.

For C-STLL, unless otherwise stated, the accuracy threshold in (22) is set to $\varphi = 0.8$, thus requiring that a fraction larger than 80% of validation data points is correctly classified. The risk tolerance in (34) is set to $\epsilon = 0.2$, so that for the selected hyperparameter λ^* the probability of meeting the accuracy requirement is at least 80%. Finally, the error level in (25) is $\delta = 0.05$, so that the probability of selecting an unreliable hyperparameter λ^* is no more than 0.05. C-STLL is run for at most $L_{\max} = 10$ iterations.

C. Benchmarks

For comparison, we consider the standard application of STLL [10], along with a number of variants of C-STLL:

STLL: This baseline learns a single STL formula by minimizing a robustness-based loss (16) over the training dataset \mathcal{D} . Unlike C-STLL, STLL does not generate a set of candidate formulas and does not employ stopping criteria and acceptance rule, and therefore provides no explicit reliability control. It is obtained from Algorithm 1 by setting $L_{\max} = 1$.

C-STLL with stopping rule only: This variant of the proposed C-STLL scheme uses the stopping rule based on the set-level quality function F , but it does not apply the complexity and diversity checks when accepting individual formulas ϕ_l . Accordingly, in this case, only the stopping threshold λ_3 is optimized, while thresholds λ_1 and λ_2 are not used in Algorithm 1.

C-STLL with complexity check and stopping rule: This variant of C-STLL enforces the complexity-based acceptance rule, admitting a candidate formula ϕ_l only if its complexity satisfies (26), but no diversity constraint is applied. In this case, only the complexity threshold λ_1 and the stopping threshold λ_3 are optimized, while threshold λ_2 is not used in Algorithm 1.

C-STLL with diversity check and stopping rule: This variant enforces the diversity-based acceptance rule, requiring each accepted formula ϕ_l to be sufficiently dissimilar from previously accepted formulas, but no complexity constraint is applied. In this case, only the diversity threshold λ_2 and the stopping threshold λ_3 are optimized, while threshold λ_1 is not used in Algorithm 1.

C-STLL with Bonferroni correction: We also consider a baseline that selects the hyperparameter λ using Bonferroni-corrected MHT as the FWER-controlling mechanism. For each $\lambda \in \Lambda$, this scheme computes the p-value in (36), and declares λ reliable if $p(\lambda) < \delta/|\Lambda|$. Therefore, the reliable set is given by $\Lambda_{\text{valid}} = \{\lambda \in \Lambda | p(\lambda) < \delta/|\Lambda|\}$, and we select the hyperparameter $\lambda^* \in \Lambda_{\text{valid}}$ that yields the smallest set size as in (38). This benchmark allows us to verify the benefits of

Pareto testing [32] as a hyperparameter selection strategy.

We emphasize that all C-STLL variants are novel, and that prior art only considered STLL [10].

D. Results

We start by considering data labeled via the ground-truth STL formula ϕ^{true} in (39). To illustrate the operation of different schemes, in Table I, we present examples of STL formula sets learned using the same dataset \mathcal{D} under STLL, which returns a single formula, as well as with the mentioned C-STLL variants. As discussed, the C-STLL variants implement different acceptance and stopping mechanisms, which directly shape the resulting set. Table I also reports the accuracy on the same validation dataset \mathcal{D}^v as in (21), i.e., $(\sum_{i=1}^{|\mathcal{D}^v|} \mathbb{1}(\hat{Y}_i = Y_i))/|\mathcal{D}^v|$, marking in bold the STL formulas with accuracy above the target threshold $\varphi = 0.8$.

STLL returns a single formula, which is quite different from the ground-truth STL formula ϕ^{true} in (39), yielding an accuracy level below the target 80%. In contrast, C-STLL results in a compact set, where each formula is both low in complexity and complementary to the others, resulting in at least one formula in the set with accuracy above the threshold φ .

When only the stopping rule is used, C-STLL admits all learned formulas until the aggregate quality criterion is met. As a result, the corresponding set is large, and contains many formulas that are structurally similar or redundant. Introducing a complexity check restricts the admission of formulas with many temporal or Boolean operators, leading to a smaller set composed of simpler and more interpretable formulas. In contrast, enforcing a diversity check suppresses formulas whose robustness behaviors are similar to previously accepted ones, encouraging structural variety but still allowing relatively complex formulas to enter the set. This analysis validates the importance of including complexity and diversity checks.

We now evaluate aggregate metrics to study the average performance of C-STLL. To this end, Fig. 4 shows the test performance of STLL and of all C-STLL variants as a function of the risk tolerance ϵ on a test set. We evaluate four key metrics, including average risk (24), average set size $|\mathcal{C}_\lambda(\mathcal{D})|$, average formula complexity (26), and average diversity (28). Recall that the risk $R(\lambda)$ measures the probability of the set $\mathcal{C}_\lambda(\mathcal{D})$ including no STL formulas above the target reliability φ . The average complexity is defined as the normalized number of temporal operations in an STL formula (see Section IV-B), while the average diversity is computed as the mean of all pairwise distances between formulas using (28).

Fig. 4(a) shows the empirical average risk achieved by each scheme on the test dataset. The dashed diagonal indicates the target constraint ϵ . STLL fails to control the risk, while all C-STLL schemes control the risk below the pre-defined tolerance ϵ , validating the effectiveness of the conformal calibration framework. The Bonferroni-based scheme consistently yields the lowest empirical risk, which is expected due to its conservative nature. In contrast, the baseline C-STLL and its variants exhibit a tradeoff between reliability and expressiveness: relaxing the selection criterion allows the

model to admit more compact or diverse formula sets at the cost of operating closer to the risk boundary.

Fig. 4(b) reports the average size of the learned STL formula set. A decreasing trend is observed for most schemes as the target ϵ increases, indicating that a looser risk tolerance allows fewer formulas while controlling the risk. C-STLL consistently produces the smallest sets, as it directly optimizes for early stopping once a sufficient quality level is reached. C-STLL with stopping-rule-only variant yields larger sets, since it lacks additional structural constraints and thus accumulates more candidate formulas before termination.

Fig. 4(c) illustrates the average normalized complexity of formulas in the selected sets. Schemes that explicitly penalize complexity achieve consistently lower complexity values. C-STLL maintains relatively low complexity due to its early-stopping mechanism. In contrast, the diversity-aware and Bonferroni-based schemes result in higher complexity on average, since diversity and conservative testing both favor retaining richer temporal structures to hedge against different failure modes.

Fig. 4(d) shows the average diversity of the learned STL sets. As expected, C-STLL with diversity check and stopping rule consistently achieves high diversity. C-STLL with complexity check and stopping rule scheme shows lower diversity than other variants, since restricting formula complexity inherently limits structural variation.

Finally, we consider the setting in which labels are assigned by an LLM-as-a-judge. Fig. 5 reports the corresponding test performance as function of the risk tolerance ϵ on the test dataset. All C-STLL variants successfully control the empirical risk below the target risk tolerance ϵ , validating the effectiveness of the proposed framework also under subjective, QoE-driven labels. Compared to Fig. 4, we observe moderately larger average set sizes and complexity values for most schemes, reflecting the increased ambiguity and variability induced by LLM-based labeling. Nevertheless, C-STLL yields the smallest sets due to its early-stopping generation approach, and the different variants of C-STLL provide relative gains that are consistent with those discussed in Fig. 4.

VI. CONCLUSIONS

This paper has introduced conformal signal temporal logic learning (C-STLL), a novel framework for extracting interpretable temporal specifications from wireless network KPI traces with formal reliability guarantees. By combining the expressiveness of STL with the distribution-free coverage guarantees of modern hyperparameter selection methods, C-STLL addresses both *relevance* – capturing temporal patterns predictive of high-level requirements such as QoE – and *interpretability* – providing human-readable specifications that network operators can validate, understand, and act upon.

The key insight behind C-STLL is to move beyond learning a single STL formula to constructing a calibrated *set* of formulas with provable guarantees. Through sequential generation with principled acceptance and stopping rules, C-STLL ensures that the returned set contains at least one formula achieving a target accuracy level with high probability. The acceptance rules, based on complexity and diversity thresholds,

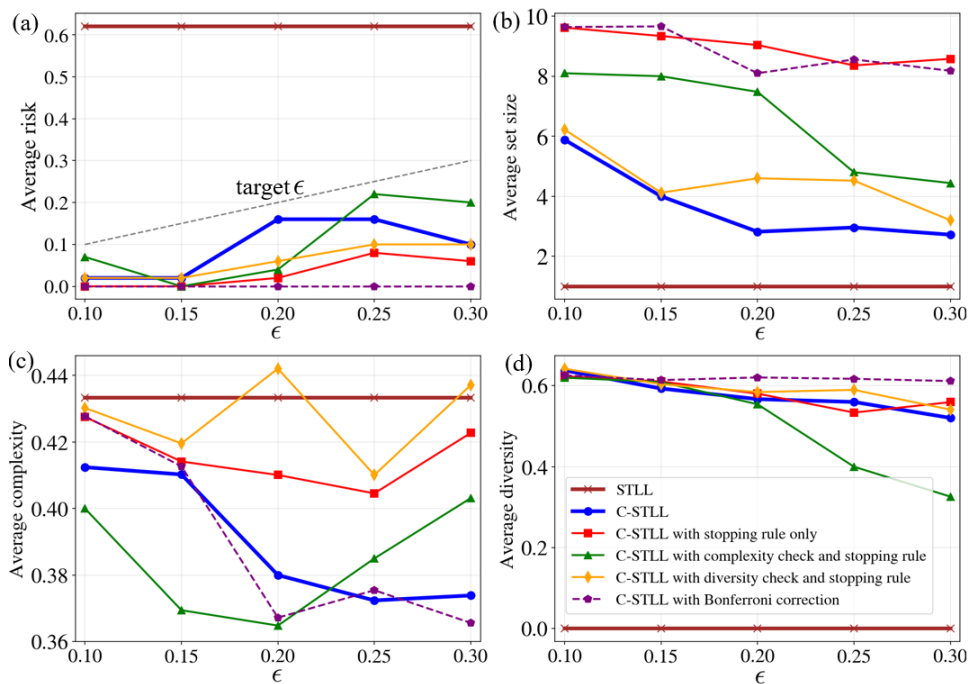


Fig. 4. Average test performance as a function of the target risk ϵ (the probability that the set $\mathcal{C}_\lambda(\mathcal{D})$ includes no STL formulas with validation accuracy above $\varphi = 0.8$) with data labeled using the ground-truth STL formula (39): (a) Average risk. (b) Average set size. (c) Average complexity (26). (d) Average diversity (28).

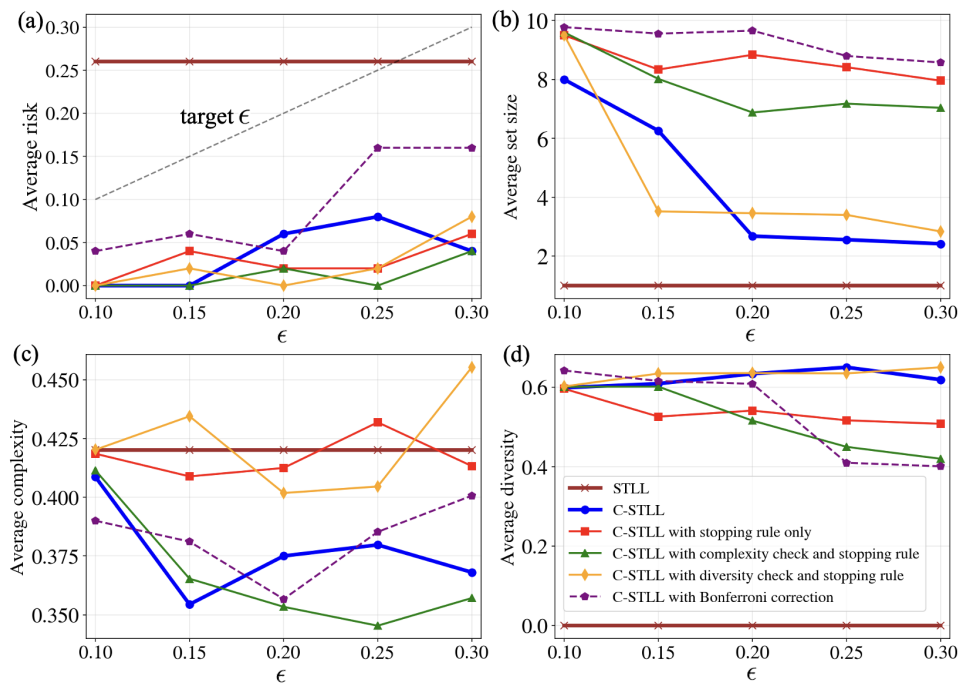


Fig. 5. Average test performance as a function of the target risk ϵ (the probability that the set $\mathcal{C}_\lambda(\mathcal{D})$ includes no STL formulas with validation accuracy above $\varphi = 0.8$) with data labeled using LLM: (a) Average risk. (b) Average set size. (c) Average complexity (26). (d) Average diversity (28).

promote interpretability by favoring simpler formulas while encouraging structural variety to capture different aspects of the underlying temporal patterns. The calibration procedure, grounded in the Learn Then Test (LTT) framework and implemented via Pareto testing followed by fixed-sequence testing [33], efficiently searches the hyperparameter space

while maintaining rigorous statistical validity.

Experimental results on a mobile gaming scenario simulated using ns-3 have demonstrated the effectiveness of C-STLL. Compared to standard STLL [10], which returns a single formula without reliability assurances, C-STLL produced compact sets of diverse, low-complexity formulas that achieved

high accuracy on validation data. Ablation studies confirmed the importance of each component: complexity checks yielded more interpretable formulas, diversity checks prevented redundancy, and the stopping rule enabled efficient early termination once sufficient quality was achieved.

Several directions merit further investigation. First, there may be QoE requirements that may be better expressed in terms of functions of the KPIs. Developing solutions that account for this, while preserving interpretability is an open challenge. Second, extending C-STLL to an *online* setting, where KPI traces arrive sequentially and the formula set must be updated incrementally, would enhance its applicability to real-time network monitoring. Third, incorporating *multi-task* learning across heterogeneous network conditions and application types could improve generalization and reduce the calibration data requirements. Fourth, Third, validating C-STLL with real QoE measurements, as well as on a real O-RAN architecture, would support practical deployment for automated KPI-to-requirement translation in softwarized networks. Finally, investigating the use of large language models to generate natural-language explanations of learned STL formulas could further bridge the gap between formal specifications and operator understanding.

APPENDIX A: TEMPORAL LOGIC INFERENCE NETWORK

This appendix reviews TLINet [10], which learns STL formulas by integrating quantitative STL semantics with neural network optimization.

vSTL Representation: TLINet uses vectorized STL (vSTL), where Boolean operators \wedge/\vee and temporal operators \square/\diamond are parameterized by binary vectors. A binary vector $\mathbf{w}_b \in \{0,1\}^n$ selects active subformulas in Boolean operations, while $\mathbf{w}_I \in \{0,1\}^T$ encodes the time interval $[t_1, t_2]$ for temporal operators, with $w_I^t = 1$ if $t_1 \leq t \leq t_2$. The robustness computations in (10)–(13) are reformulated accordingly over these binary vectors.

TLINet Architecture: As illustrated in Fig. 3, TLINet contains predicate, temporal, and Boolean modules arranged in layers. The predicate module takes trajectory \mathbf{X} as input and outputs robustness vectors using trainable parameters \mathbf{a} and \mathbf{b} . Temporal modules learn the interval bounds t_1, t_2 via smooth approximations of \mathbf{w}_I , and select between \square and \diamond using a Bernoulli variable κ with trainable probability p_κ . Boolean modules similarly learn subformula selection via Bernoulli variables for \mathbf{w}_b and operator type, either \wedge or \vee , via another Bernoulli variable κ_b . The output robustness $\rho(\mathbf{X}, \phi, 0)$ serves as the decision score. The training objective combines the hinge classification loss in (16) with regularizers promoting binarization of all probabilities via $p(1-p)$ terms and sparsity in Boolean selection via ℓ_1 regularization on p_b . Parameters are optimized using stochastic gradient descent.

APPENDIX B: LTT VIA PARETO TESTING

The calibration set \mathcal{D}^{cal} is partitioned into $\mathcal{D}_1^{\text{cal}}$ with K_1 pairs for Pareto testing and $\mathcal{D}_2^{\text{cal}}$ with K_2 pairs for fixed-sequence testing.

Pareto testing: For each candidate $\lambda \in \Lambda$, we run C-STLL on $\mathcal{D}_1^{\text{cal}}$ to compute the empirical risk

$$\hat{R}(\lambda, \mathcal{D}_1^{\text{cal}}) = \frac{1}{K_1} \sum_{k=1}^{K_1} \mathbb{1}(\#\phi \in \mathcal{C}_\lambda(\mathcal{D}_{k,1}) : A(\phi, \mathcal{D}_{k,1}^v) = 1)$$

and average set size

$$|\mathcal{C}_\lambda(\mathcal{D}_1^{\text{cal}})| = \frac{1}{K_1} \sum_{k=1}^{K_1} |\mathcal{C}_\lambda(\mathcal{D}_{k,1})|.$$

Since risk and set size are conflicting objectives, solving the multi-objective problem $\min_{\lambda} \{\hat{R}(\lambda, \mathcal{D}_1^{\text{cal}}), |\mathcal{C}_\lambda(\mathcal{D}_1^{\text{cal}})|\}$ yields a Pareto frontier $\bar{\Lambda} \subseteq \Lambda$. The hyperparameters in $\bar{\Lambda}$ are then ordered by increasing p-values as defined in (36).

Fixed-sequence testing: Using $\mathcal{D}_2^{\text{cal}}$, we test the ordered hyperparameters sequentially. For each $\lambda_{\pi(i)}$, we compute the empirical risk

$$\hat{R}(\lambda_{\pi(i)}, \mathcal{D}_2^{\text{cal}}) = \frac{1}{K_2} \sum_{k=1}^{K_2} \mathbb{1}(\#\phi \in \mathcal{C}_{\lambda_{\pi(i)}}(\mathcal{D}_{k,2}) : A(\phi, \mathcal{D}_{k,2}^v) = 1),$$

and its p-value

$$p(\lambda_{\pi(i)}) = \Pr(b(K_2, \epsilon) \leq K_2 \hat{R}(\lambda_{\pi(i)}, \mathcal{D}_2^{\text{cal}})).$$

The hypothesis in (34) is rejected if $p(\lambda_{\pi(i)}) < \delta$. Testing proceeds until the first non-rejected hypothesis at index $\pi(i^*)$, yielding $\Lambda_{\text{valid}} = \{\lambda_{\pi(1)}, \dots, \lambda_{\pi(i^*-1)}\}$. The final selection $\lambda^* \in \Lambda_{\text{valid}}$ minimizes the average set size $|\mathcal{C}_{\lambda^*}(\mathcal{D}_2^{\text{cal}})|$.

APPENDIX C: PROOF OF THEOREM 1

The reliability condition (25) follows from the validity of the p-value in (36) combined with the FWER control of fixed-sequence testing.

To show that the p-value is valid, let $S = |\mathcal{D}^{\text{cal}}| \hat{R}(\lambda, \mathcal{D}^{\text{cal}})$ and note that $S \sim b(|\mathcal{D}^{\text{cal}}|, R(\lambda))$ since calibration pairs are i.i.d. For any $\alpha \in [0, 1]$, because the binomial CDF $F_\epsilon(\cdot)$ is nondecreasing, the event $\{F_\epsilon(S) \leq \alpha\}$ implies $S \leq c_\alpha$, where c_α is the α -quantile index. Under the null hypothesis (34), the binomial CDF is nonincreasing in its success probability, so $\Pr(S \leq c_\alpha) \leq F_\epsilon(c_\alpha) \leq \alpha$. This confirms the inequality $\Pr(p(\lambda) \leq \alpha | \mathcal{H}_\lambda) \leq \alpha$.

Since fixed-sequence testing controls the FWER at level δ [40], with probability at least $1 - \delta$ no true null hypothesis is rejected, and the selected λ^* satisfies the reliability condition (25).

REFERENCES

- [1] B. Brik, A. Ksentini, and M. Bouaziz, “Deep learning for B5G open radio access network: Evolution, survey, case studies, and challenges,” *IEEE Open Journal of the Communications Society*, vol. 3, pp. 228–250, 2022.
- [2] M. Polese, L. Bonati, S. D’Oro, S. Basagni, and T. Melodia, “Understanding O-RAN: Architecture, interfaces, algorithms, security, and research challenges,” *IEEE Communications Surveys & Tutorials*, vol. 25, no. 2, pp. 1376–1411, 2023.
- [3] L. Bonati, M. Polese, S. D’Oro, S. Basagni, and T. Melodia, “Intelligence and learning in O-RAN for data-driven NextG cellular networks,” *IEEE Communications Magazine*, vol. 59, no. 10, pp. 21–27, 2021.

- [4] A. Lacava, M. Polese, R. Sivaraj, R. Soundararajan, B. S. Bhati, T. Singh, T. Zugno, F. Cuomo, and T. Melodia, "Programmable and customized intelligence for traffic steering in 5G networks using open RAN architectures," *IEEE Transactions on Mobile Computing*, vol. 23, no. 4, pp. 2882–2897, 2024.
- [5] W. Guo, "Explainable artificial intelligence for 6G: Improving trust between human and machine," *IEEE Communications Magazine*, vol. 58, no. 6, pp. 39–45, 2020.
- [6] B. Brik, K. Boutiba, and A. Ksentini, "Explainable AI in 6G O-RAN: A tutorial and survey on architecture, use cases, challenges, and future directions," *IEEE Communications Surveys & Tutorials*, vol. 26, no. 4, pp. 2490–2520, 2024.
- [7] C. Fiandrino, L. Bonati, S. D'Oro, M. Polese, T. Melodia, and J. Widmer, "EXPLORA: AI/ML explainability for the open RAN," *Proceedings of the ACM on Networking*, vol. 1, no. CoNEXT3, pp. 1–26, 2023.
- [8] O. Maler and D. Nickovic, "Monitoring temporal properties of continuous signals," in *International symposium on formal techniques in real-time and fault-tolerant systems*, pp. 152–166, Springer, 2004.
- [9] A. Donzé and O. Maler, "Robust satisfaction of temporal logic over real-valued signals," in *Proc. FORMATS*, pp. 92–106, Springer, 2010.
- [10] D. Li, M. Cai, C.-I. Vasile, and R. Tron, "TLINet: Differentiable neural network temporal logic inference," *arXiv preprint arXiv:2405.06670*, 2024.
- [11] G. Bombara, C.-I. Vasile, F. Penber, H. Yasuoka, and C. Belta, "Offline and online learning of signal temporal logic formulae using decision trees," *ACM Transactions on Cyber-Physical Systems*, vol. 5, no. 3, pp. 1–23, 2021.
- [12] G. E. Fainekos and G. J. Pappas, "Robustness of temporal logic specifications for continuous-time signals," *Theoretical Computer Science*, vol. 410, no. 42, pp. 4262–4291, 2009.
- [13] E. Bartocci *et al.*, "Specification-based monitoring of cyber-physical systems: A survey on theory, tools and applications," *Handbook of Runtime Verification*, pp. 135–175, 2018.
- [14] L. Panizo, M.-d.-M. Gallardo, F. Luque-Schempp, and P. Merino, "Runtime monitoring of 5G network slicing using STAn," *Journal of Logical and Algebraic Methods in Programming*, vol. 145, p. 101059, 2025.
- [15] A. Adadi and M. Berrada, "Peeking inside the black-box: A survey on explainable artificial intelligence (XAI)," *IEEE Access*, vol. 6, pp. 52138–52160, 2018.
- [16] D. Luan and J. Thompson, "Channelformer: Attention based neural solution for wireless channel estimation and effective online training," *IEEE Transactions on Wireless Communications*, vol. 22, no. 10, pp. 6562–6577, 2023.
- [17] O. T. Basaran and F. Dressler, "XAI-on-RAN: Explainable, airtight, and gpu-accelerated RAN towards 6G," *arXiv preprint arXiv:2511.17514*, 2025.
- [18] F. Rezazadeh, H. Chergui, and J. Mangués-Bafalluy, "Explanation-guided deep reinforcement learning for trustworthy 6G ran slicing," in *Proc. IEEE international conference on communications workshops*, pp. 1026–1031, 2023.
- [19] O. T. Basaran and F. Dressler, "Xainomaly: Explainable and interpretable deep contractive autoencoder for o-ran traffic anomaly detection," *Computer Networks*, vol. 261, p. 111145, 2025.
- [20] L. Malakalapalli, V. Gudepu, B. Chirumamilla, S. Yadhunandan, and K. Kondepu, "Integrating explainable ai for energy efficient open radio access networks," in *Proc. IEEE Future Networks World Forum*, pp. 232–237, 2024.
- [21] V. Vovk, A. Gammerman, and G. Shafer, *Algorithmic Learning in a Random World*. 2005.
- [22] G. Shafer and V. Vovk, "A tutorial on conformal prediction," *Journal of Machine Learning Research*, vol. 9, pp. 371–421, 2008.
- [23] K. Cohen, S. Park, O. Simeone, and S. Shamai, "Calibrating AI models for wireless communications via conformal prediction," *IEEE Transactions on Machine Learning in Communications and Networking*, vol. 1, pp. 296–312, 2023.
- [24] K. Cohen, S. Park, O. Simeone, P. Popovski, and S. Shamai, "Guaranteed dynamic scheduling of ultra-reliable low-latency traffic via conformal prediction," *IEEE Communications Letters*, vol. 27, no. 5, pp. 1473–1477, 2023.
- [25] O. Simeone, S. Park, and M. Zecchin, "Conformal calibration: Ensuring the reliability of black-box AI in wireless systems," *arXiv preprint arXiv:2504.09310*, 2025.
- [26] J. Chen, S. Park, P. Popovski, H. V. Poor, and O. Simeone, "Neuromorphic split computing with wake-up radios: Architecture and design via digital twinning," *IEEE Transactions on Signal Processing*, vol. 72, pp. 4635–4650, 2024.
- [27] F. Caioli, L. Bortolussi, J. V. Deshmukh, L. Lindemann, and N. Paoletti, "Conformal predictive monitoring for multimodal scenarios," in *Proc. International Conference on Runtime Verification*, pp. 336–356, 2025.
- [28] A. N. Angelopoulos, S. Bates, E. J. Candès, M. I. Jordan, and L. Lei, "Learn then test: Calibrating predictive algorithms to achieve risk control," *The Annals of Applied Statistics*, vol. 19, no. 2, pp. 1641–1662, 2025.
- [29] A. A. Barakabitze, A. Ahmad, R. Mijumbi, and A. Hines, "QoE management of multimedia streaming services in future networks: A tutorial and survey," *IEEE Communications Surveys & Tutorials*, vol. 22, no. 1, pp. 526–565, 2020.
- [30] P. Charonyktakis, M. Plakia, I. Tsamardinos, and M. Papadopoulou, "On user-centric modular QoE prediction for VoIP based on machine-learning algorithms," *IEEE Transactions on Mobile Computing*, vol. 15, no. 6, pp. 1443–1456, 2016.
- [31] G. Kougioumtzidis, V. Poulkov, P. Lazaridis, and Z. Zaharis, "Deep learning-aided QoE prediction for virtual reality applications over open radio access networks," *IEEE Access*, vol. 11, pp. 143514–143529, 2023.
- [32] B. Laufer-Goldshtein, A. Fisch, R. Barzilay, and T. Jaakkola, "Efficiently controlling multiple risks with pareto testing," *arXiv preprint arXiv:2210.07913*, 2022.
- [33] V. Quach, A. Fisch, T. Schuster, A. Yala, J. H. Sohn, T. S. Jaakkola, and R. Barzilay, "Conformal language modeling," *arXiv preprint arXiv:2306.10193*, 2023.
- [34] A. Donzé, "On signal temporal logic," in *Proc. International conference on runtime verification*, pp. 382–383, 2013.
- [35] O. Simeone, *Machine Learning for Engineers*. Cambridge University Press, 2022.
- [36] M. A. Ganaie, M. Hu, A. K. Malik, M. Tanveer, and P. N. Suganthan, "Ensemble deep learning: A review," *Engineering Applications of Artificial Intelligence*, vol. 115, p. 105151, 2022.
- [37] L. V. Jospin, H. Laga, F. Boussaid, W. Buntine, and M. Benamoun, "Hands-on bayesian neural networks—a tutorial for deep learning users," *IEEE Computational Intelligence Magazine*, vol. 17, no. 2, pp. 29–48, 2022.
- [38] G. Bombara, C.-I. Vasile, F. Penedo, H. Yasuoka, and C. Belta, "A decision tree approach to data classification using signal temporal logic," in *Proc. International Conference on Hybrid Systems: Computation and Control*, pp. 1–10, 2016.
- [39] C. Madsen, P. Vaidyanathan, S. Sadraddini, C.-I. Vasile, N. A. DeLateur, R. Weiss, D. Densmore, and C. Belta, "Metrics for signal temporal logic formulae," in *Proc. IEEE Conference on Decision and Control (CDC)*, pp. 1542–1547, 2018.
- [40] B. L. Wiens, "A fixed sequence bonferroni procedure for testing multiple endpoints," *Pharmaceutical Statistics: The Journal of Applied Statistics in the Pharmaceutical Industry*, vol. 2, no. 3, pp. 211–215, 2003.
- [41] H. Li, Q. Dong, J. Chen, H. Su, Y. Zhou, Q. Ai, Z. Ye, and Y. Liu, "LLMs-as-judges: a comprehensive survey on llm-based evaluation methods," *arXiv preprint arXiv:2412.05579*, 2024.
- [42] J. Gu *et al.*, "A survey on LLM-as-a-judge," *The Innovation*, 2024.